Decomposition of complex movements into primitives for Parkinson's disease assessment

E. K. Pissadaki
A. G. S. Abrami
S. J. Heisig
E. Bilal
M. Cavallo
P. W. Wacnik
K. Erb
D. R. Karlin
P. R. Bergethon
S. P. Amato
H. Zhang
V. L. Ramos
F. Hameed
J. J. Rice

Recent advances in technology present an important opportunity in medicine to augment episodic, expert-based observations of patients' disease signs, obtained in the clinic, with continuous and sensitive measures using wearable and ambient sensors. In Parkinson's disease (PD), such technology-based objective measures have shown exciting potential for passively monitoring disease signs, their fluctuation, and their progression. We are developing a system to passively and continuously capture data from people with PD in their daily lives, and provide a real-time estimate of their motor functions, that is analogous to scores obtained during Part III of the human-administered Movement Disorder Society's Unified Parkinson's Disease assessment (MDS-UPDRS3). Our hypothesis is that complex human movements can be decomposed into movement primitives related to the performance of the MDS-UPDRS3 motor assessment. Toward this hypothesis, we developed a system for integrating and analyzing multiple streams of sensor data collected from volunteers executing the tasks based on the MDS-UPDRS3. In this paper, we show how we can leverage the data collected from MDS-UPDRS3 tasks to develop machine learning models that can identify movement primitives in activities of daily living.

Introduction

Estimating the progress of neurodegenerative diseases depends largely on episodic observations during clinical visits and estimating how these observables deviate from a healthy state. A medical system where assessment, therapeutic intervention, and restoration to a healthy state are based on real time and a continuous flow of health-related information [1] is now conceivable. Using wearable and ambient sensors, one can acquire user-generated data and derive technology-based objective measures (TOMs) to form a closed-loop system of medical care [2], which attempts to mimic the natural homeostatic behaviors of an organism to increase wellness and well-being of an individual [3].

Parkinson's disease (PD) is a neurodegenerative disease that affects over a million persons living in the United States and has rapidly growing social and economic impact [4]. PD, as a neurological movement disorder, makes an excellent disease model for applying TOMs, which have the potential to provide more continuous, sensitive, and objective measures than the current standard approaches based on human examiners [5]. Selective degeneration of dopaminergic neurons in the substantia nigra *pars compacta* [6] results in the principal motor signs of the disease (we prefer the term "sign," which can be detected by outside observer, to the term "symptom," which is only experienced by the individual affected by the disease): bradykinesia (slowness of movement), rigidity (stiffness and resistance to passive movement), and tremor, and gait and balance difficulties [7]. There is no cure for the disease, and treatment is based on managing symptoms, primarily, but not exclusively, in the form of dopamine replacement.

The Movement Disorder Society's Unified Parkinson's Disease Rating Scale, specifically part III with a focus on motor examination (MDS-UPDRS3), is a standardized assessment of the motor signs of PD [8]. This is among the most commonly used clinical research instruments [9, 10] to quantify PD signs and disease progression [9]. However, the MDS-UPDRS3 has limitations; It is an episodic assessment

Digital Object Identifier: 10.1147/JRD.2017.2768739

that requires expert training to have high test-retest reliability [11], and generally the subject must travel to a clinic. A goal in the field is to develop continuous TOMs that are less disruptive to normal activities of people with Parkinson's (PwP). Such continuous measures could potentially allow subtle differentiation between phenotypes of the disease, refine medication intake, and improve sensitivity and specificity in monitoring disease progression [12].

Substantial work has already been done to develop TOMs in PD. Electromyograms (EMGs), electrocardiograms (ECG), electroencephalograms, wearable inertial sensors, and audio sensors for phonetic analysis have been used to provide continuous, objective measures of the motor and non-motor aspects of PD [13, 14]. Prior research in this field include home monitoring of PwP via wearable technology [15], automatic detection of fluctuations between the OFF state and the ON state using inertial sensors [16], and quantification of bradykinesia by sensor fusion while performing bradykinesia-related tasks of the MDS-UPDRS3 assessment [17]. Patients report being in the OFF state when disease symptoms are at their worst, with severe bradykinesia, rigidity, and tremor, whereas when patients are treated with dopamine and regain control of movements towards the normal state, this is called the ON state. A strong association between kinematic features extracted from a subset of MDS-UPDRS3 tasks and scores using inertial measurements units (IMU) sensors has previously been reported by Parisi and colleagues [18]. Similarly, Piro et al. [19] compare the MDS-UPDRS3 ratings using a single classifier, namely the pronation-supination classifier, on the basis of a 3D animated human avatar.

Our objective is to develop a continuous assessment of motor function analogous to the one obtained from MDS-UPDRS3. We aim to create a set of MDS-UPDRS3-task-derived classifiers with which human activities in real life will be decomposed and expressed as a function of these simpler motor signatures that facilitate automation and qualification. These motor signatures are referred to here as "movement primitives." For this proof-of-concept study, we describe our methodology to collect, store, analyze, and classify movement primitives and show that they can be extracted during scripted activities of daily living (ADLs). The methodology developed is part of a larger project to improve data collection and patient assessment in clinical trials, ultimately aimed at developing personalized, closed-loop therapies in difficult-to-manage diseases such as PD.

Materials and methods

Motivation

We performed an observational research study on healthy volunteers to develop a dataset of time series segments of human activity that corresponds to elements of the UPDRS3 motor examination and motor aspects of activities of daily living. Healthy volunteers were recruited to participate by executing the study experimental protocol, while the methods and data collection pipelines were being tested and refined. The healthy volunteers' data served as the control group to compare with respect to the test group, i.e., data collected from PwP executing the same experimental protocol. Herein, we present the methodology applied to recognize human activity in the form of motor primitives based on UPDRS3 tasks performed by the control group of healthy volunteers.

Sensors

Three different device types were used in our experimental set up: a) Biostamp Research Connect (BiostampRC) system by MC10, Inc., b) Opal version one devices manufactured by Ambulatory Parkinson's Disease Monitoring (APDM) wearable technology company, and c) Kinect v2 motion capture device manufactured by Microsoft. All data streams were resampled, aligned, and stored in a relational database (described further below) with the appropriate metadata for each participant and session.

BiostampRC is a multi-sensor device designed to collect biometric signals in a flexible silicon package that is applied to the body surface with adhesives. Each sensor device contains a low-power three-axis accelerometer, a high-range six-axis gyroscope and accelerometer, and an analog front end for surface EMGs and ECG measurement. Data are stored in its local memory and then can be transferred wirelessly to other devices. Advantages of using BiostampRC sensors include easy placement in various body locations and the ability to simultaneously record EMG, ECG, and kinematic data. A sampling frequency of 250 Hz is used for all data in our studies.

The Opal sensor device comprises a single-package wearable IMU with a three-axis accelerometer, a three-axis gyroscope, and a three-axis magnetometer. Advantages of using APDM Opals include the ability to stream kinematic data from multiple sensors at a high sampling rate (128 Hz) and within the same wireless network using a wireless access point that synchronizes all IMUs. The APDM Mobility Lab software output timestamped tuples include linear acceleration, angular velocity, and magnetic field strength in comma separated values (CSV) format. Quaternions are also reported, enabling reconstruction of the absolute orientation in space of each sensor in Earth coordinates. APDM Mobility Lab software computes 98 features of gait, balance, and postural sway, and these features are used, along with our own custom-defined features, as input to our machine learning algorithms to classify the performance of MDS-UPDRS3 tasks.

Kinect v2, a successor of the Microsoft Kinect, is a multipurpose device containing different types of sensors and designed for use in the video gaming industry. Our study requires a subset of the device's functionalities for video recording and motion tracking capabilities. In addition

to the common 1,080 p resolution color camera (30 frames per second [FPS]), the device provides an infrared-based depth camera with 512×424 resolution. Image processing algorithms, based on machine learning, extract human skeletal location data. Kinect v2 can track up to 6 different skeletons simultaneously for persons located within a 70° horizontal field of view (FOV) with a range of 0.8 m to approximately 4 m from the sensor. Skeletal location data consist of 3D spatial information collected from up to 25 human joints recorded at 30 FPS through custom-made software, and this enables the storage of both color video and data in the form of a CSV file. Note that we have deployed Kinect in our laboratory studies because of the ease of use in collecting skeletal location data to calibrate the wearable sensor systems. However, limitations in range and FOV, as well as privacy concerns of placing cameras in homes, may limit the applicability to deployment in subjects' living environments in future studies.

ETL and SNOMED-based database

The Extract, Transform, and Load (ETL) process was guided by each device's siloed tool chain that needed to be accommodated. We implemented software to extract data from the various proprietary application programming interfaces (APIs) and formats for each device type. The Systematized Nomenclature of Medicine Clinical Terms (SNOMED CT) [20] is a global clinical terminology that supports clinical data capture and effective retrieval and reuse of clinical information. This semantically driven and interoperable ontology is aligned with standardized labels to identify the demographic data, and we additionally use the ontology terms to capture the associated symptomatology, to identify anatomic location of movements and sensor placement, and to describe the MDS-UPRDS3 and prescribed ADL tasks. Our approach may eventually be extended and interface with existing ontologies systems such as the Semantic Sensor Network Ontology (SSNO) for describing sensors and the observations for diverse applications, including large-scale scientific monitoring, industrial and home monitoring, and the Internet of Things [21]. SSNO also facilitates the development of specialized ontologies to complement data capturing workflows and to apply ontologically driven metadata for precise machine learning.

A record was kept for each data collection session with the Cmed Encapsia eSource application [22]. This application recorded labels for each task occurring during the sessions with the corresponding timestamps that result from human data entry events. These label data were extracted from the Encapsia eSource application and passed forward to our database with time alignment with the sensor data. Each device type had a different time format, so all devices must be reconciled to a common time format before the data could be aligned. Ultimately the time series sensor data with the label timestamps, subject demographic, experimenter, and environmental data were loaded into a MariaDB relational database.

Participants

We studied healthy participants prescreened and recruited by Pfizer, Inc. (Andover, MA, USA) and the IBM T. J. Watson IBM Research Center (Yorktown Heights, NY, USA) research sites—following an open call for volunteers. We enrolled $n = 60$ participants, 33 female (average age 45.91 ± 11.00, years $\pm$ std) and 27 male (average age 42.23 ± 10.30, years $\pm$ std), from 24 to 70 years old (average age 44.29 ± 10.77, years $\pm$ std). All subjects were healthy male and female subjects with no clinically relevant abnormalities, physically able, and willing to participate with the study procedures, as identified by subject self-report and investigator assessment. All subjects signed informed consent before participating in the study. The study protocol was approved by the Schulman Independent Institutional Review Board (Schulman IRB#201500837).

Each subject participated in a study consisting of two sessions of approximately 60 minutes each, either recorded during a single subject visit or divided into two visits. Hence, a total of 120 sessions were collected from the subject pool.

Protocol

Upon completing intake procedures, trained examiners positioned six APDM Opals and eight MC10 BiostampRC sensors, as shown in **Figure 1(a).** BiostampRC sensors were positioned on the lateral shanks, left thigh, the ventral aspect of the forearm over the right and left flexor digitorum, the dorsal aspect of the forearm over the right and left extensor digitorum, and on the chest over the heart. The chest sensor recorded the ECG in addition to IMU data. The arm sensors recorded EMG plus IMU data, and the other devices provided only IMU data streams. Opal sensors were positioned at the participants' feet, wrists, lumbar region of the lower back, and sternum. Sensors were held in place by straps with Velcro fasteners. Data from APDM Opal sensors were collected via a custom wireless protocol, whereas the MC10 BiostampRC data transferred to a mobile Android tablet and then to a proprietary cloud.

Participants were instructed to execute the series of 13 movement tasks, contained in the MDS-UPDRS3. In brief, an examiner tested for: a) rigidity by passively moving body parts across major joints with the participant in a relaxed position; and b) bradykinesia by asking the participant to tap their index finger to their thumb, flex and extend their hands, and pronate-supinate their hands, and tap their toes and stomp their feet on the ground using maximum speed and excursion for 10 repetitions. Both the dominant then non-dominant sides were examined. Gait, balance and postural stability were measured by repetitive

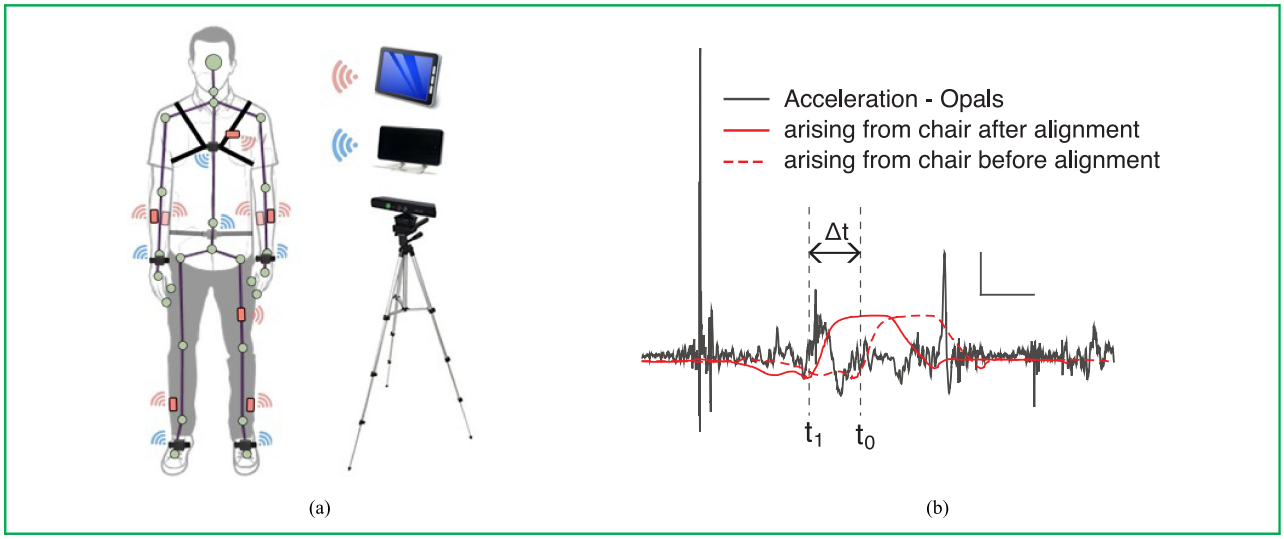

Figure 1

Sensor placement and example of acquired signals. (a) Participants were equipped with six APDM Opals (shown by black ovals) and eight MC10 BiostampRC (shown by red rectangles). Microsoft Kinect v2, a motion-tracking device, reports the position of 24 skeletal locations (shown by green dots). (b) Example of time alignment needed for fusion heterogeneous sensor tracks. An arising-from-chair protocol is performed to produce motion-tracking data from the Microsoft Kinect v2 device signal at the sternum (red trace) overlaid with acceleration signal from an Opal device (black trace). The hardware infrastructures are not synchronized, so a shift of $\Delta t = 1.287$ s is required as shown (dash red trace) to time align the signals. Scale bars are as follows: vertical (2.5 m/s^2) and horizontal (2 s).

standing and sitting, and gait evaluation with turning, and stability of stance under the duress of a sudden and forceful pull on the shoulders. Participants also completed tasks normally used to evaluate the presence and severity of rest tremor, kinetic tremor (asking the participant to alternatively touch their own nose and then the finger of the examiner), and postural tremor (asking the participant to hold arms outstretched). The examination protocol was complemented by five additional movement-related subtasks (see bold font in **Table 1**). In addition, the protocol included 14 scripted ADLs, which were timestamped for later retrieval and analysis. All participants performed the same series of scripted ADLs while the aforementioned system of sensors recorded their movements. Examples of ADL routines included: a) untying and tying shoelaces, b) opening and closing a door, or c) putting on a lab coat and buttoning, unbuttoning, and removing the coat.

Table 1 Motor examination tasks. Healthy volunteers execute a complete set of the MDS-UPRDS3, complemented by five additional movement-related subtasks (bold font): a) sit to stand with arms crossed; b) five repetitions (referred to as 5x) of sit to stand with arms crossed; c) 30 s postural sway during quiet stance with eyes open; d) similar but with eyes closed; e) rotation, 360° turn test. Each side (dominant and non-dominant hand and leg) is examined separately.

Rigidity	*Hands*	*Legs*	*Sit to stand*	*Posture*	*Gait*	*Postural stability*	*Tremor*
Slow passive movement of major joints (five tasks)	Finger tapping 10 s and 90 s	Toe tapping 10 s and 90 s	Using chair arms	**30 s eyes open, arms side**	3m walk x3	Response to sudden body displacement	Postural tremor
	Flexion-extension 10 s and 90 s	Leg agility 10 s and 90 s	**With arms crossed**	**30 s eyes closed, arms hip**	10 m walk		Finger to nose
	Pronation-supination 10 s and 90 s		**5x arms crossed**	**Rotation**	2 min walk		Rest tremor

Table 2 Frequency of responses to the survey performed after the end of the second session. The first number is the number of respondents, and the second is the percent of the total = 60.

Item						
1. Overall comfort (range: 0 to 5)	*0*	*1*	*2*	*3*	*4*	*5*
APDM	0 – 0%	0 – 0%	2 – 3.3%	8 – 13%	25 – 41%	25 – 41%
BiostampsRC	0 – 0%	0 – 0%	1 – 1.6%	3 – 5%	10 – 16%	46 – 75%
2. Continuous monitoring at home for multiple days	*Very unlikely*	*Unlikely*		*Likely*	*Very likely*	
APDM	4 – 6.5%	11 – 18%		25 – 41%	20 – 33%	
BiostampRC	1 – 1.6%	5 – 8%		20 – 33%	34 – 56%	
3. Sensors locations that were particularly uncomfortable	APDM sternum 14 – 23%	APDM Left wrist 2 – 3%	APDM Right wrist 5 – 8%		APDM Lumbar 7 – 12%	APDM Left foot 1 – 1.6%
	BiostampRC Chest 2 – 3%	BiostampRC Thigh 2 – 3%	BiostampRC Ventral forearms 3 – 5%		BiostampRC Dorsal forearms 2 – 3%	

Wearability of sensors

An important component in using remote monitoring is the user acceptability of the wearable sensors for short or long periods of monitoring time [23]. To assess comfort and acceptability in our study, we conducted a questionnaire survey at the end of the second experimental session for all subjects $(n = 60)$. Six of the questionnaire's items are presented in **Table 2**. In item 1, subjects rated comfort for wearing the sensors, with zero indicating that they were uncomfortable but tolerable enough to participate in the study, and five indicating that the sensors were so comfortable so as to be unnoticeable during the study. We assessed their willingness to wear the sensors continuously at home for multiple days (item 2) and whether there were particular sensor locations that were uncomfortable (item 3). Overall, BiostampRC sensors were rated as more comfortable to wear, and have had fewer location discomfort reports as compared to the APDM sensors. Our analysis is limited to fairly short-term use in a clinical study within a research site. Further studies will be needed to understand wearability issues for continuous wear in the home or public settings for which other issues such as self-consciousness can arise.

Data curation

We aligned each data set according to the following procedure. The delay between the APDM and BiostampRC IMU data streams and the motion-sensing skeleton data was characterized by maximizing the cross correlation of the three signals. The time alignment process is shown in Figure 1(b) depicting the "arising from chair" MDS-UPDRS3 task used as a reference point to synchronize all data stream. Each MDS-UPDRS3 task was manually timestamped in real experimental time by a manual key press, a process that potentially introduces errors and sub-optimal separation between the meaningful signal from noise. We developed a semi-supervised procedure that detected the most relevant start–end time points for each MDS-UPDRS3 task. This automated procedure was required because there were often delays between the cuing by examiner and the actual performance of the tasks by the subject. In other cases, extraneous actions occurred before or after the desired task. By removing irrelevant data in the stored MDS-UPDRS3 segmented tasks, we reduce the occurrence of confounding noise, which can substantially degrade classification accuracy by machine learning techniques.

Machine learning algorithm and classification

Sensor data collected during the 13 MDS-UPDRS3 and six complementary tasks were labeled as shown in the content of Table 1. Of the pool of 19 labeled tasks, 11 have been used to train the classifiers of the current study so far. For example, for one classifier, we used the "Posture eyes open" and "Posture eyes closed" tasks (in which the subject stood still for both) as training data for sedentary behavior. For flexion-extension and grasping behavior, the training data was the "flexion-extension" and "finger tapping" tasks (specifically, dominant and non-dominant hand performed for 10 s and non-dominant hand performed for 90 s). For pronation-supination behavior, the training data were the "pronation-supination" task (dominant and non-dominant hand for 10 s and non-dominant hand for 90 s). To develop the classifiers, the MDS-UPDRS3-task data were segregated in training sets (70% of data) and test sets (remaining 30% of data). Once the classifiers were trained to detect primitives in the

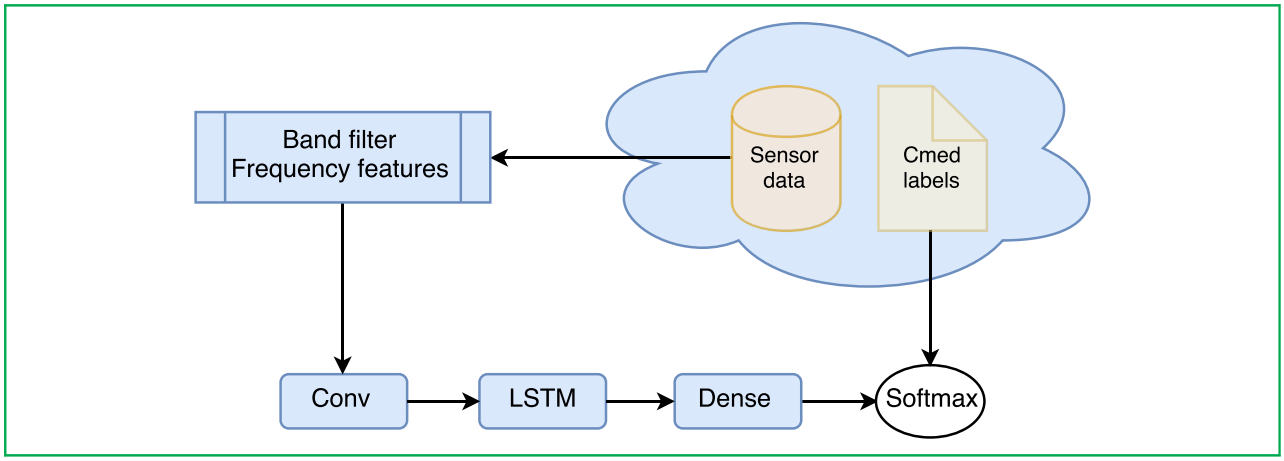

Figure 2

Architecture of the neural network (NN). The upper part of the figure concerns feature generation: A band filter is applied to the time-series data to remove the gravity component from the accelerometers and other low-frequency artifacts caused by events like walking. The time domain is then transformed to the frequency domain using a fast Fourier transform that is then fed into the convolutional layer. The lower part of the figure concerns the main NN architecture. The NN is composed of four layers, a 1-D convolutional layer, an LSTM layer, a dense layer, and a softmax layer where the class probabilities are generated.

MDS-UPDRS3-task data, the same classifiers were run to extract primitives in the scripted ADL time-series data.

The raw signals from x-, y-, and z-axis accelerometer and gyroscope data streams were pre-processed to correct for sampling rate variation and sensor noise by using cubic-spline interpolation followed by Butterworth bandpass filtering. Time-series data were split into equal length segments using a sliding window. Each window was then processed using the fast Fourier transform to extract the amplitudes of the frequencies across the sampling spectrum. These features were fed into a neural network architecture composed of a one-dimensional convolutional layer with rectified linear unit (ReLU) nonlinearity, followed by a long short-term memory (LSTM) layer, and finally one dense layer with ReLU nonlinearities. The convolutional layer was down-sampled by max pooling, and standard dropout regularization was applied between the layers; see **Figure 2** for a schematic representation. Following training using the Kingma and Ba version of stochastic gradient descent [24], we found that the frequency-based features that performed best when the convolutions were calculated across the ordered frequency domain as opposed to the time domain. Specifically, for each time window, frequency amplitudes were extracted using a fast Fourier transform. The convolutional filter is then applied across the extracted amplitudes that are sorted in ascending order by corresponding frequency.

Results

We have developed a flexible relational database structure that allows data to be extracted, visualized, and analyzed based on arbitrary combinations of labels for tasks, body location, sensor type, subject demographics, etc. Because data are stored as time-aligned and trimmed sequences, these analyses can be performed with greater ease than working with the raw data streams. **Figure 3** illustrates the capabilities that are enabled by this infrastructure. Panel A shows an example of a time series extracted from the database of acceleration signals measured during the pronation-supination task in our protocol. Each subject performed 10 repetitions of pronation-supination movement using both the dominant and non-dominant hand while wearing the sensor set previously described. Panel B shows an example summary of angular velocity (i.e., rotation speed) data acquired by the gyroscopes from Opal sensors positioned on the wrists. Data were extracted for right-handed volunteers and the maximum angular velocity was computed during the pronation-supination task. Data are shown as separate distributions for the dominant (green) and non-dominant hands (blue). The two hands showed similar distributions (Kruskal Wallis test, $p = 0.0797 > 0.05$), and for each session, dominant vs. non-dominant hands showed no difference ($n = 71$, Wilcoxon signed rank test, $p = 0.0989 > 0.05$). With our database approach, similar analyses could be easily performed based on other criteria, e.g., as a function of age, first vs. second session, left-handed vs. right-handed subjects, etc.

We also demonstrated an example of another key aspect of our approach. Here, we showed that a scripted ADL task that entails a complex series of motor activities could be decomposed to movement primitives derived from the MDS-UPDRS3 tasks. As illustrated by the sequence in

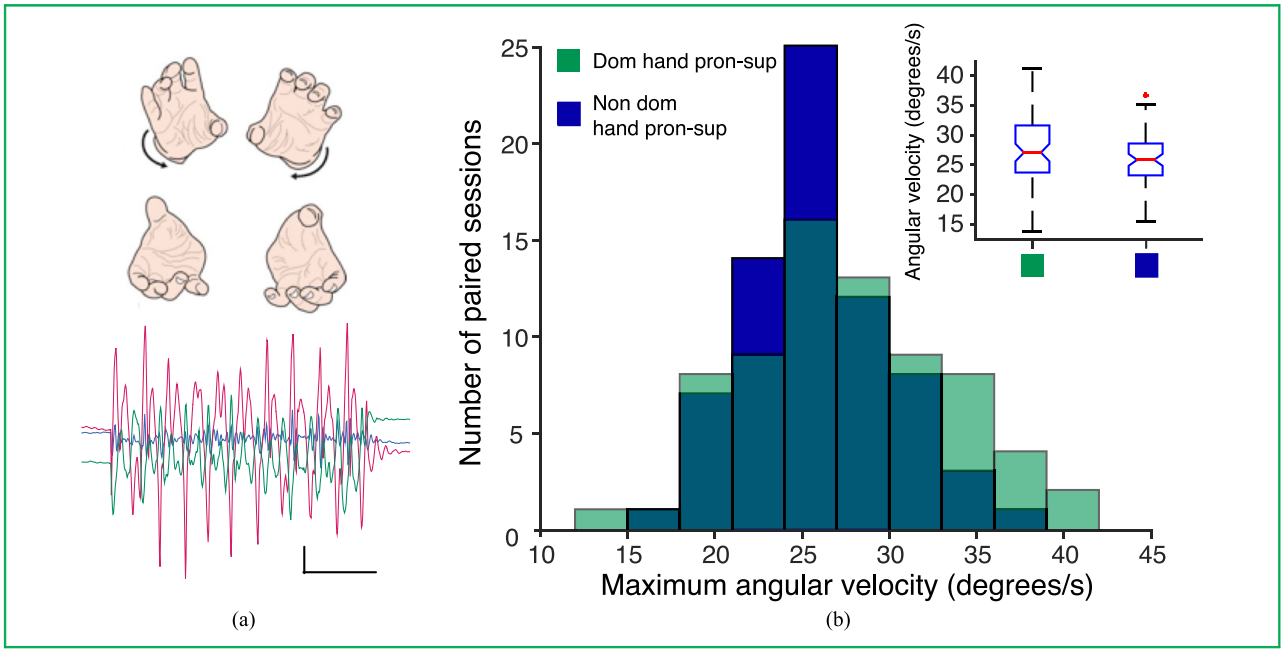

Figure 3

Sample data and analytics for the pronation and supination task. (a) The upper panel illustrates the pronation-supination of the hand. The lower panel shows representative acceleration signals in three axes for the pronation-supination task. For the scale bars, the vertical line corresponds to 10 m/s^2, and the horizontal line to 1 s. (b) Distribution of the maximum angular velocity as measured by the x-axis gyroscope and computed for 71 sessions with right-handed participants performing the pronation-supination task. Green bars correspond to the dominant (right) and blue bars to the non-dominant hand (left). The inset boxplots depict the median maximum angular velocity for each case. Upper left panel depicting the pronation-supination task was adapted from https://clinicalgate.com/ with permission from the author.

Figure 4, the scripted ADL task required the participant to start from a static standing position, walk toward a door, reach out for a lab coat on a hook, put the lab coat on, button all the buttons, unbutton all, and then take the lab coat off. We trained a classifier to produce a running estimate of the probability during defined windows of the occurrence of two primitives: flexion-extension and pronation-supination. The classifier assumed that the subject is sedentary when not performing either of the other two tasks, so that the probability is equal to one minus the other two probabilities in any given window.

Figure 4 shows an example of the output from this classifier for one subject performing an ADL task. The algorithm predicts a high probability of being sedentary for the first 18 seconds while the subject was mostly standing in place. Then sedentary probability decreases and flexion-extension probability increases as the subject was reaching out for the lab coat from 18 seconds to ~27 seconds. Next, the probability of pronation-supination increases as the subject was buttoning up the lab coat from 27 seconds to 29 seconds. From this point onwards, the flexion-extension and pronation-supination classes showed mutually complementary pattern of high probabilities as the subject was repeatedly grasping and twisting the button during both the buttoning and unbuttoning phases of the scripted ADL. A human-annotated description of the activities is shown at the lower panel of Figure 4, with coloring corresponding to the primitives showing highest probabilities. This example supports our initial hypothesis that complex ADL movement can be decomposed into movement primitives based on MDS-UPDRS3 tasks. However, further testing over the entire set of ADLs will be required to consolidate this preliminary result.

Discussion

We describe a methodology for capturing, fusing, storing, and analyzing sensor data from healthy volunteers performing MDS-UPDRS3 tasks. Using machine learning on labeled data, we can construct classifiers to detect the occurrence of movement primitives in testing data sets. We show an example case in which the primitives are extracted from the right-hand IMU sensor data stream from a healthy volunteer performing a scripted ADL. Hence, we have demonstrated a proof of concept for an approach of automatically extracting primitives from complex motor patterns.

Substantial evidence exists demonstrating the ability of kinematic measurements made using body-worn sensors during the performance of MDS-UPDRS3 tasks to predict physician-assigned scores [15, 19, 25–28]. Typically,

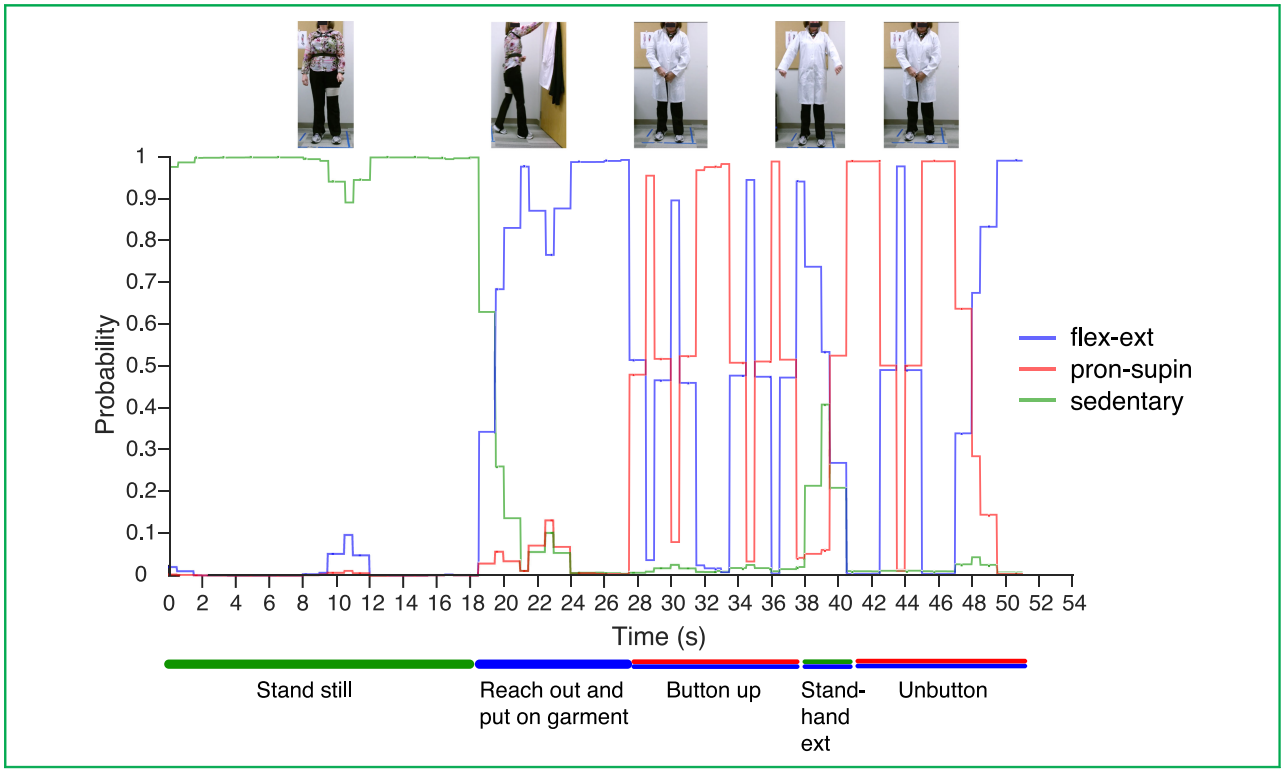

Figure 4

Human activity recognition based on MDS-UPDRS3-derived primitives. The subject performs a scripted ADL of standing, walking to pick up a coat off a hook, putting on the garment, and buttoning and then unbuttoning (see small sample photos in upper panel). The outputs of classifiers trained on the primitive activities are shown in the central panel (red: flexion-extension, annotated as flex-ext; blue: pronation-supination, annotated as pron-supin; and green: sedentary). The lower panel shows a timeline of the participant's movement activity, labeled by human annotation, with colors indicating the primitives with high probabilities, as determined by the classifiers, during the periods shown.

features derived from the data are used to compute a predictor of the UPDRS as scored by a human. For example, Stamatakis and colleagues used a regression model to automatically predict UPDRS test scores derived from the finger-tapping task [25]. Similarly, Piro et al. [19] used support vector machines to automatically classify UPDRS, using the pronation-supination task. Along the same lines, Giuberti and colleagues investigated how kinematic data collected from a single MDS-UPDRS3 task, sit to stand, can be representative of the MDS-UPDRS3 score assigned by a neurologist [28].

Our approach differs in several respects from previous work. While many early studies showed derived features correlate with MDS-UPDRS3, in most cases, the feature space is based on heuristics or is predefined based on prior knowledge [29]. In some of the approaches, the machine learning chooses the most predictive set of features from the predefined space (e.g., [30]). In contrast, we are attempting to use a data-driven approach in which machine learning chooses the features from the primary sensor data without user input or prior knowledge. A potential downside to this approach is that the training set may need to be large, a requirement that could be challenging with the size of datasets often collected with human studies. Our strategy is to initially collect a large number of sensor streams with a goal of winnowing down to the most informative, under the assumptions that only a few sensors can be reliably deployed in the real-world setting of continuous tracking in subjects' homes. We plan to use machine learning as a tool for dimensionality reduction to assist in minimizing the number of sensors deployed to assess PD.

Our approach to decompose ADLs into movement primitives extracted from MDS-UPDRS3 tasks has not been reported before to our knowledge. We hypothesize that this approach may provide important insights that might be missed by using more global and composite features (e.g., energy within specific spectral frequency bands without considering the specific context). Analyses based on movement primitives will inherently consider a context based on body location and movement sequence. Moreover, assessed primitives may map more directly to brain areas than other global and composite features. For example, hand movements map to underlying brain circuitry [31, 32], and hand configurations may be organized into a limited number

of components [29] in a low-dimensional manner, with four to five dimensions being sufficient to explain 80%–90% of the variability in natural movement data [33]. Along these lines, a primitive-based approach may provide a more direct mapping to the affected regions of the brain and potentially could more precisely define the phenotype of the given patient. Indeed, MDS-UPDRS3-based assessment revealed that PwP cluster into several phenotypes [34, 35] that may reflect underlying difference in the disease pathophysiology.

While we demonstrated the initial framework, much work remains to be done toward the goal of assessing PwP in a manner than recapitulates that of a human examiner. To that end, we need to train classifiers to both *detect* movement primitives and *score* movement primitives on the MDS-UPDRS scale. We are now collecting sensor data from PwP who are performing MDS-UPDRS3 tasks with scores derived from human raters. Ideally, we will have different subjects providing example data over the range of possible scores, typically from normal motion ($score = 0$) to highly degraded performance ($score = 4$). From these data, we can construct a training set for which a classifier could learn to rate the primitives. If successful in both detecting and scoring primitives in the controlled setting of a MDS-UPDRS3 test, then the same classifiers could be applied to PwP performing normal activities during everyday life.

Conclusion

We implemented a methodology to capture, store, curate, and retrieve for analysis data from body-worn sensors generated during the performance of MDS-UPDRS3 tasks and then construct machine learning classifiers of movement primitives. We demonstrate a proof of concept that complex movements such as ADLs can be automatically decomposed into movement primitives in healthy volunteers. Further work will be required to show that automatic classification will be as successful in context of the tremor, bradykinesia, rigidity and gait/balance disturbances that can occur in PD. Moreover, we will be constructing additional classifiers to rate degree that performance of primitives is degraded in PD so that a score can be automatically assigned that is analogous to a human rater. While the current studies are limited to data from healthy volunteers, the results show progress toward a goal of automated and continuous activity quantification and monitoring in PD.

Acknowledgment

We thank David Caouette of Pfizer and Robert Stackhouse, Christine Kretz and Ajay Royyuru of IBM Research for their managerial support of this research project.

References

1. K. Shameer, M. A. Badgeley, R. Miotto, et al., "Translational bioinformatics in the era of real-time biomedical, health care and wellness data streams," *Brief Bioinformat.*, vol. 18, no. 1, pp. 105–124, Jan. 2017.
2. C. Zrenner, P. Belardinelli, F. Muller-Dahlhaus, et al., "Closed-loop neuroscience and non-invasive brain stimulation: A tale of two loops," *Front Cell Neurosci.*, vol. 10, no. 92, 2016.
3. L. Hood and C. Auffray, "Participatory medicine: A driving force for revolutionizing healthcare," *Genome Med.*, vol. 5, no. 12, 2013.
4. R. T. Scheife, G. T. Schumock, A. Burstein, et al., "Impact of Parkinson's disease and its pharmacologic treatment on quality of life and economic outcomes," *Amer. J. Health Syst. Pharmacy*, vol. 57, no. 10, pp. 953–962, May 15, 2000.
5. A. J. Espay, P. Bonato, F. B. Nahab, et al., "Technology in Parkinson's disease: Challenges and opportunities," *Movement Disorders*, vol. 31, no. 9, pp. 1272–1282, Sep. 2016.
6. W. R. Gibb and A. J. Lees, "Anatomy, pigmentation, ventral and dorsal subpopulations of the substantia nigra, and differential cell death in Parkinson's disease," *J. Neurol., Neurosurg., Psychiatry*, vol. 54, no. 5, pp. 388–396, 1991.
7. J. Jankovic, "Parkinson's disease: Clinical features and diagnosis," *J. Neurol. Neurosurg. Psychiatry*, vol. 79, no. 4, pp. 368–376, Apr. 2008.
8. C. G. Goetz, B. C. Tilley, S. R. Shaftman, et al., "Movement disorder society-sponsored revision of the unified Parkinson's disease rating scale (MDS-UPDRS): Scale presentation and clinimetric testing results," *Movement Disorders*, vol. 23, no. 15, pp. 2129–2170, Nov. 15, 2008.
9. J. S. Perlmutter, "Assessment of Parkinson disease manifestations," *Current Protocols Neurosci.*, ch. 10, unit 10.1, Oct. 2009.
10. C. Ramaker, J. Marinus, A. M. Stiggelbout, et al., "Systematic evaluation of rating scales for impairment and disability in Parkinson's disease," *Movement Disorders*, vol. 17, no. 5, pp. 867–876, Sep. 2002.
11. A. Siderowf, M. McDermott, K. Kieburtz, et al., "Test-retest reliability of the unified Parkinson's disease rating scale in patients with early Parkinson's disease: Results from a multicenter clinical trial," *Movement Disorders*, vol. 17, no. 4, pp. 758–763, Jul. 2002.
12. C. Godinho, J. Domingos, G. Cunha, et al., "A systematic review of the characteristics and validity of monitoring technologies to assess Parkinson's disease," *J. Neuroeng. Rehabil.*, vol. 13, Mar. 12, 2016.
13. Q. W. Oung, H. Muthusamy, H. L. Lee, et al., "Technologies for assessment of motor disorders in Parkinson's disease: A review," *Sensors (Basel)*, vol. 15, no. 9, pp. 21710–21745, Aug. 31, 2015.
14. M. Pastorino, M. T. Arredondo, J. Cancela et al., "Wearable sensor network for health monitoring: The case of Parkinson disease," *J. Phys., Conf. Ser.*, vol. 450, no. 1, 2013, Art. no. 012055.
15. S. Patel, B. R. Chen, T. Buckley et al., "Home monitoring of patients with Parkinson's disease via wearable technology and a web-based application," in *Proc. Conf. IEEE Eng. Med. Biol. Soc.*, 2010, vol. 2010, pp. 4411–4414.
16. C. Pérez-López, A. Samà, D. Rodríguez-Martín, et al., "Monitoring motor fluctuations in Parkinson's disease using a waist-worn inertial sensor," in *Advances in Computational Intelligence* (13th International Work-Conference on Artificial Neural Networks, IWANN 2015, Palma de Mallorca, Spain, June 10–12, 2015. Part I), I. Rojas, G. Joya and A. Catala, Eds. Cham, Switzerland: Springer-Verlag, 2015, pp. 461–474.
17. E. R. O. Martinez-Manzanera, M. Beudel, R. W. K. Borgemeester, et al., "A method for automatic and objective scoring of Bradykinesia using orientation sensors and classification algorithms," *IEEE Trans. Biomed. Eng.*, vol. 63, no. 5, pp. 1016–1024, May 2016.
18. F. Parisi, G. Ferrari, M. Giuberti, et al., "Body-sensor-network-based kinematic characterization and comparative outlook of UPDRS scoring in leg agility, sit-to-stand, and gait tasks in Parkinson's disease," *IEEE J. Biomed. Health Informat.*, vol. 19, no. 6, pp. 1777–1793, Nov. 2015.
19. N. E. Piro, L. K. Piro, J. Kassubek, et al., "Analysis and visualization of 3D motion data for UPDRS rating of patients with Parkinson's disease," *Sensors (Basel)*, vol. 16, no. 6, Jun. 21, 2016.

20. T. Benson, *Principles of Health Interoperability HL7 and SNOMED*. London, U.K.: Springer-Verlag, 2012.
21. K. S. Taylor, K. Janowicz, D. Le Phuoc, et al., "Semantic sensor network ontology." [Online]. Available: https://www.w3.org/TR/vocab-ssn/
22. "Cmed Encapsia clinical data suite." [Online]. Available: http://www.cmedresearch.com/28-encapsia-clinical-data-suite.html
23. J. M. Fisher, N. Y. Hammerla, L. Rochester, et al., "Body-worn sensors in Parkinson's disease: Evaluating their acceptability to patients," *Telemed. J. E-Health*, vol. 22, no. 1, pp. 63–69, Jan. 2016.
24. D. P. Kingma and J. L. Ba, "ADAM: A method for stochastic optimization," in *Proc. 3rd Int. Conf. Learn. Representations*, San Diego, CA, USA, 2015.
25. J. Stamatakis, J. Ambroise, J. Cremers, et al., "Finger tapping clinimetric score prediction in Parkinson's disease using low-cost accelerometers," *Comput. Intell. Neurosci.*, vol. 2013, 2013, Art. no. 717853.
26. D. A. Heldman, D. E. Filipkowski, D. E. Riley, et al., "Automated motion sensor quantification of gait and lower extremity Bradykinesia," in *Proc. Conf. IEEE Eng. Med. Biol. Soc.*, 2012 vol. 2012, pp. 1956–1959.
27. S. Patel, H. Park, P. Bonato, et al., "A review of wearable sensors and systems with application in rehabilitation," *J. Neuroeng. Rehabil.*, vol. 9, no. 21, Apr. 20, 2012.
28. M. Giuberti, G. Ferrari, L. Contin, et al., "Automatic UPDRS evaluation in the sit-to-stand task of Parkinsonians: Kinematic analysis and comparative outlook on the leg agility task," *IEEE J. Biomed. Health Informat.*, vol. 19, no. 3, pp. 803–814, May 2015.
29. E. Kim, S. Helal, and D. Cook, "Human activity recognition and pattern discovery," *IEEE Pervasive Comput.*, vol. 9, no. 1, pp. 48–53, Jan.–Mar. 2010.
30. R. J. Lemmens, Y. J. Janssen-Potten, A. A. Timmermans, et al., "Recognizing complex upper extremity activities using body worn sensors," *PLoS One*, vol. 10, no. 3, 2015, Art. no. e0118642.
31. H. Shibasaki, N. Sadato, H. Lyshkow, et al., "Both primary motor cortex and supplementary motor area play an important role in complex finger movement," *Brain*, vol. 116 (Pt 6), pp. 1387–1398, Dec. 1993.
32. S. T. Witt, A. R. Laird, and M. E. Meyerand, "Functional neuroimaging correlates of finger-tapping task variations: an ALE meta-analysis," *Neuroimage*, vol. 42, no. 1, pp. 343–356, Aug. 1, 2008.
33. J. J. Belic and A. A. Faisal, "Decoding of human hand actions to handle missing limbs in neuroprosthetics," *Front. Comput. Neurosci.*, vol. 9, no. 27, 2015.
34. W. J. Zetusky, J. Jankovic, and F. J. Pirozzolo, "The heterogeneity of Parkinson's disease: Clinical and prognostic implications," *Neurology*, vol. 35, no. 4, pp. 522–526, Apr. 1985.
35. R. J. Uitti, Y. Baba, Z. K. Wszolek, et al., "Defining the Parkinson's disease phenotype: Initial symptoms and baseline characteristics in a clinical cohort," *Parkinsonism Related Disorders*, vol. 11, no. 3, pp. 139–145, May 2005.

Received April 4, 2017; accepted for publication May 4, 2017

Eleftheria K. Pissadaki *IBM Research, T. J. Watson Research Center, Yorktown Heights, NY 10598 USA (ekpissad@us.ibm.com).* Dr. Pissadaki holds a B.S. degree in mathematics, an M.Sc. degree in neuroscience, and a Ph.D. degree in computational neuroscience from the University of Crete, Greece. She currently works as a Neuroscientist in the Computational Biology Center at the IBM T. J. Watson Research Center. Prior to her appointment at IBM, Dr. Pissadaki was a Researcher at the University of Oxford, spearheading research on the etiopathology of Parkinson's disease while being awarded a Parkinson's UK Innovation Grant and the MRC Centenary Career Award. Her scientific interests include dopamine neuron physiology, hippocampal dynamics, signal analysis, and biophysical compartmental modeling.

Avner G. S. Abrami *IBM Research, T. J. Watson Research Center, Yorktown Heights, NY 10598 USA (avner.abrami@ibm.com).* Mr. Abrami is a Researcher and Data Scientist in the Computational Biology Center at the IBM T. J. Watson Research Center. He received his B.S. degree in applied mathematics from Ecole Centrale Paris in 2015, and an M.S. degree in operations research from Columbia University in 2016. He applies his expertise in applied mathematics, machine learning, optimization and signal processing related projects.

Stephen J. Heisig *IBM Research, T. J. Watson Research Center, Yorktown Heights, NY 10598 USA (heisig@us.ibm.com).* Mr. Heisig graduated from Rensselaer Polytechnic Institute with a B.S. degree in computer science. He then joined IBM and worked in the system test organization debugging problems until joining the Systems department of the research division in 1997. His current work in the Computational Biology Center is related to phenotypic surveillance and characterizing human traits in disease states.

Erhan Bilal *IBM Research, T. J. Watson Research Center, Yorktown Heights, NY 10598 USA (ebilal@us.ibm.com).* Dr. Bilal is a Researcher in the Multiscale System Biology and Modeling group at IBM's Computational Biology Center, as well as an affiliate member of Sage Bionetworks. He received M.Sc. and B.S. degrees in automatic control and industrial informatics from the Politehnica University of Bucharest in Romania, and a Ph.D. degree in computational biology from Rutgers University. His research is focused on the application of big data analytics to the development of biomarkers and therapeutic strategies in cancer and the use of wearable sensors for the assessment of motor function state.

Marco Cavallo *IBM Research, Thomas J. Watson Research Center, Yorktown Heights, NY 10598 USA (mcavall@us.ibm.com).* Mr. Cavallo is a Data Scientist in the Computational Biology Center at the IBM T. J. Watson Research Center. He received an M.S. degree in computer science from the University of Illinois at Chicago in 2016 and, during the same year, an M.Eng. degree in computer engineering from Politecnico di Milano, Italy. He joined IBM at the T. J. Watson Research Center during Fall 2016 to pursue research in data visualization and develop visual analytics tools. His research interests also extend to the augmented and virtual reality domains.

Paul W. Wacnik *Early Clinical Development; Pfizer R&D, Cambridge, MA 02139 USA (paul.wacnik@pfizer.com).* Dr. Wacnik is a Clinician and Director in the Digital Medicine department at Pfizer R&D in Cambridge. He received a B.S. degree in mechanical engineering from Purdue University, and a Ph.D. degree in neuroscience and pharmacology from the University of Minnesota. He first joined Medtronic R&D and then Medical Affairs at Pfizer in the Neuroscience and Pain group. He currently leads collaborative research projects at several academic centers. He is author or coauthor of several patents and 31 manuscripts and book chapters.

Kelley Erb *Early Clinical Development, Pfizer Inc., Cambridge, MA 02139 USA (michaelkelley.erb@pfizer.com).* Dr. Erb received a B.S. degree in mechanical engineering from Lehigh University in 2004 and a Ph.D. degree in Anatomy and Neurobiology from the Boston University School of Medicine in 2012. At Pfizer, he leads the technical development of novel digital endpoints for the continuous monitoring of health states in movement disorders populations. Prior to arriving at Pfizer, he worked as an engineer in the defense industry and drove product development and clinical study execution at an early stage medical device company.

Daniel R. Karlin *Early Clinical Development, Pfizer Inc., Cambridge, MA 02139 USA (daniel.karlin@pfizer.com).* Dr. Karlin is a Psychiatrist and Medical Informatician at Pfizer, where he is the Head of Experimental Medicine and Regulatory Strategy for the Pfizer

Innovation Research Laboratory. He received a B.A. degree in neuroscience and behavior, and an M.A. degree in medical informatics from Columbia University, and he received his M.D. degree from the University of Colorado.

Peter R. Bergethon *Cambridge, MA 02139 USA (peter.bergethon@biogen.com).* Dr. Bergethon is a Neurologist and led the Pfizer Innovation Research Laboratory. He currently leads Quantitative Medicine and Clinical Technologies at Biogen, Inc. He earned an M.D. degree from Jefferson Medical College, trained at the Boston City Hospital, and is board certified in both internal medicine and neurology. Before joining Pfizer, he was a Professor of anatomy and neurobiology at Boston University School of Medicine. Dr. Bergethon has been awarded the Founder's Award from the American Academy of Neurology and authored or contributed to over 100 research papers and books. His research interest is focused on computational modeling of the underlying structural organization and biophysical mechanisms in the nervous system.

Stephen P. Amato *Pfizer Worldwide Research and Development, Cambridge, MA 02139 USA (stephen.amato@pfizer.com).* Dr. Amato is a Project Manager in the Early Clinical Development unit within Pfizer Worldwide Research and Development. He received his B.S. degree from the State University of New York at New Paltz in 2005, and a Ph.D. degree in biology from Boston University in 2012, where he was granted the Belamarich Award for outstanding doctoral research. He joined Pfizer in 2012, where he worked on identifying and validating novel drug targets before taking on the role as Project Manager within Pfizer's Quantitative and Digital Medicine group.

Hao Zhang *Early Clinical Development, Pfizer Inc. Cambridge, MA 02139 USA* (hao.zhang2@pfizer.com). Dr. Zhang is currently a Senior Manager (Biomedical Engineering) in the Early Clinical Development unit in Pfizer. In his previous research, he studied dynamic activities of the brain. He completed a Postdoctoral Fellowship at Pfizer Neuroscience with Dr. Michael Ehlers. Prior to joining Pfizer, he obtained his Ph.D. degree in neurobiology from Duke University under the mentorship of Dr. Miguel Nicolelis. Dr. Zhang has received scholarships and awards from Duke University, Marine Biological Laboratory, Cold Spring Harbor Laboratory, and Wellcome Trust (UK). He has coauthored many scientific papers and serves as reviewer for multiple neuroscience journals.

Vesper L. Ramos *Early Clinical Development, Pfizer Inc. Cambridge, MA 02139 USA (vesper.ramos@pfizer.com).* Dr. Ramos is a movement disorders Neurologist in the Early Clinical Development unit in Pfizer. She trained at the Human Motor Control Section at the National Institutes of Health, where she focused on motor physiology and aging research, and worked as a Senior Staff Fellow-Medical Officer at the Office of Device Evaluation at the Center for Devices and Radiologic Health at the FDA, where she focused on neurological device development. She is certified by the American Board of Psychiatry and Neurology and a member of the American Academy of Neurology.

Farhan Hameed *Early Clinical Development Pfizer Inc, Cambridge, MA 02155 USA (farhan.hameed@pfizer.com).* Dr. Hameed is a Clinical Informatician in the Pfizer Innovative Research Lab. He received medical degrees (M.D./M.B.B.S.) from Dow University of Health Sciences, and an M.S. degree in health informatics from the Northeastern University. After completing his training in psychiatry at the Institute of Behavioral Sciences, he pursued a full-time career in health informatics, developed multiple clinical decision support systems (C.D.S.S.), and led development of pharmacy informatics systems for multiple hospital-based electronic health record systems. He also held adjunct positions as an Associate Professor at the College of Pharmacy at Chicago State University and Midwestern University, and currently at Northeastern University. He is an active member of several healthcare and IT organizations, the American Medical Informatics Association, and the American College of Healthcare Executives and Health Level-7, and he is a fellow of the Healthcare Information and Management Systems Society.

John J. Rice *IBM Research, Thomas J. Watson Research Center, Yorktown Heights, NY 10598 USA (johnrice@us.ibm.com).* Dr. Rice is a Principle Research Staff Member in the Computational Biology Center at the IBM T. J. Watson Research Center. He received a B.E.S. degree in biomedical engineering from Johns Hopkins University in 1987, and M.E.S. and Ph.D. degrees in 1989 and 1998, respectively. He joined IBM at the T. J. Watson Research Center in 2000 to pursue research in functional genomics, systems biology, and multiscale modeling. He is author or coauthor of 4 patents and 54 technical papers. Dr. Rice is a member of the adjunct faculty at Johns Hopkins University and Loyola University Chicago.